WASHINGTON UNIVERSITY IN ST. LOUIS

School of Engineering and Applied Science

Department of Computer Science and Engineering

Thesis Examination Committee:
Dr. Ron Cytron
Dr. Tao Ju
Dr. Robert Pless

USING REGRESSION TECHNIQUES TO PREDICT WEATHER SIGNALS FROM IMAGE SEQUENCES

by

Richard Speyer

A thesis presented to the School of Engineering
of Washington University in partial fulfillment of the
requirements for the degree of

MASTER OF SCIENCE

May 2009
Saint Louis, Missouri

ABSTRACT OF THE THESIS

Using Regression Techniques to Predict Weather Signals from Image Sequences

by

Richard Speyer

Master of Science in Computer Science

Washington University in St. Louis, 2009

Research Advisor: Dr. Robert Pless

Webcams are cheap sensors that capture a potentially large amount of information about a scene. This thesis considers the use of regression and correlation techniques such as Canonical Correlation Analysis (CCA) to convert these webcams into environmental sensors and predict the values of weather signals. Local environmental properties often directly affect the images we collect from the webcams; whether it is cloudy or sunny is visible by the presence of shadows; wind speed and direction is visible in smoke, flags, or close up views of trees; particulate density is reflected in haziness and the color spectrum during sunset. Using the AMOS database, which has been archiving nearly 1,000 webcams every 30 minutes for the last 3 years, we explore relationships between the amount of training data and the accuracy with which we are able to infer the values of certain weather signals including wind speed & direction and vapor pressure from inherent properties in the image. This allows the webcams *already* installed across the earth to act as generic sensors to improve our understanding of local weather patterns and variations.

Acknowledgments

First and foremost, I would like to thank Dr. Robert Pless, who has been my research and faculty adviser for the last four years. His constant attention and guidance have been crucial in the construction of this thesis and I am extremely grateful for all of his help. My experience working under him in the Media & Machines Lab is one of the most valuable of my college career and has taught me skills that I will surely use after I graduate.

I would also like to thank Nathan Jacobs and many other students who helped review this thesis and the related research as well as Dr. William Smart and Dr. Ron Cytron for sitting on my Thesis Committee along with Dr. Pless.

Finally, I would like to thank the Department of Computer Science & Engineering for promoting and providing many opportunities for undergraduates to get involved in research projects. I have benefited greatly from working in a research lab during my time here and that would not have been possible without the department's commitment to undergraduate research.

Richard Speyer

Washington University in Saint Louis
May 2009

Contents

List of Figures

Chapter 1

Introduction

The appearance of a scene can often give us an abundance of information about the scene including time of day, location, and weather. With all of this information available, it is up to us to find ways to automatically extract it from images of the scene to allow us to better understand what is going on at a given location. In this thesis we will attempt to use the information collected by webcams to infer information about environmental signals such as wind speed & direction and vapor pressure.

The challenge is that images may vary more due to other causes such as time of day than those which relate to our signals of interest. Thus, we begin by exploring mechanisms for learning features that are invariant to other scene changes. Through the use of correlation techniques such as Canonical Correlation Analysis (CCA), we find that we are able to extract useful information from webcam images which allow us to predict local weather data and as a result gain better understanding of local weather patterns and variations and fill in missing weather data entries, which occur quite frequently. Furthermore, this allows us to use the abundantly existing webcams all over the country as crude weather sensors instead of depending only on the government weather stations sparsely spread out across the country.

This thesis will go through the background information, motivation, and related work in Section 1. It will then discuss the theory and details of the correlation techniques used in Section 2. Section 3 will begin to show the application and results of the aforementioned methods. It will also show how we further utilize our results to determine the appropriate size of the training set necessary to avoid any inherent bias in the images. We will conclude in Section 4 and propose future work on this problem in Section 5.

1.1 Related Work

The work presented in this paper is primarily related to two areas of research in computer vision; here we will present some of the work related to algorithms designed to operate on webcam image sequences as well as the use of CCA and other correlation techniques to extract external signals from time-varying image sequences.

TODO

1.2 Background Information

The Archive of Many Outdoor Scenes (AMOS) database [5] has been collecting images from 835 webcams every 30 minutes since March 2006 and now contains over 40 million images. The AMOS dataset is unique in providing time-stamped images from many cameras around the world. No other dataset provides the broad range of geographic locations and the long temporal duration.This database is the largest known collection of natural scenes collected from static cameras and as such offers a wealth of data to test our methods against. While there are cameras located across the world, we focus on those located within the continental United States so that we can collect accurate ground truth weather data.

Our weather data is collected from the Historical Weather Data Archives (HWDA) [10] which is maintained by the National Oceanic and Atmospheric Administration (NOAA), which is an official government organization. The archives maintain a large variety of weather data from the since January 1, 1933 through present day on just over 6,000 weather stations across the continental United States. The data collected includes, but is not limited to, wind speed & direction, precipitation, temperature, relative humidity, vapor pressure, cloud conditions, dew point, and various aggregated data signals.

Chapter 2

Canonical Correlation Analysis (CCA)

The main correlation technique which we will explore is a method called Canonical Correlation Analysis (CCA) [3]. The goal of CCA is to find two transformation matrices A and B to maximize the correlation between two independent data sets $X \in \mathbf{R}^{x \times n}$ and $Y \in \mathbf{R}^{y \times n}$. In other words, CCA looks to find A and B such that $AX \approx BY$. CCA is a way of finding a linear relationship between two independent, multidimensional variables.

MORE, EQUATIONS ETC, EXPLANATION OF MULTIPLE DIMENSIONS

What makes CCA different from other correlation methods is its invariance to affine transformations of the input variables. In other words, CCA will be able to find a linear relationship between two multidimensional variables even if different coordinate systems are used for each variable [2]. This makes CCA a very desirable method for relating image data to environmental signals, which are clearly not measured in the same coordinate system. One very crucial component of CCA is that while the input matrices X and Y can have a varying number of dimensions, they must have *exactly* the same number of samples in order to find an accurate correlation between the two time-varying signals.

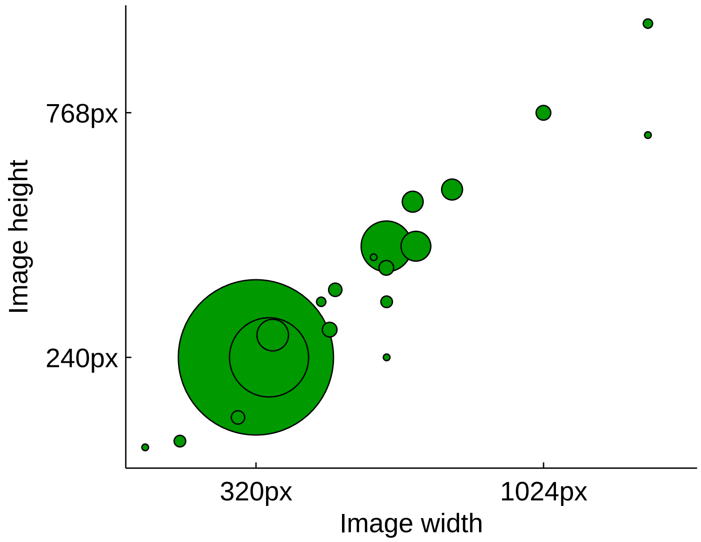

Figure 2.1: The distribution of image sizes, measured in pixels. The circles are centered at the width and height of the image and their sizes are proportional to the number of webcams which output images of that size in the AMOS dataset.

2.1 Applications

We will now focus on the application of CCA to predicting time-varying weather signals from image sequences over the same time period. Given the localized nature of weather data, we assume that the weather station used for ground truth weather data is located near to the camera in order to maximize the accuracy of our predictions. The algorithm takes as input a set of images $I = i_1 \dots i_a$ and a set of weather observations $W = w_1 \dots w_b$. The method will assume the availability of images and weather data with corresponding timestamps. In order to ensure that this invariant holds, the first step of our algorithm is to run through both data sets and remove entries that do not have a corresponding entry in the other dataset. This step guarantees that all of our data samples match and that there are an equal number in both sets, which is required for CCA. Our input is now of the form $I = i_1 \dots i_n$ and $W = w_1 \dots w_n$.

Once our datasets are properly aligned, we turn our attention to the images. Figure 2.1 shows us that the most common size image from a webcam in the AMOS dataset is 320×240 pixels, which means that we can express n image as a $n \times 76800$ matrix. This is clearly a very costly and inefficient way to store image data, especially when we are looking to run CCA with a few hundred images. In order to reduce the storage size for each image, and as a result accelerate the runtime of our algorithms, we will run Principal Component Analysis (PCA) on the images as a way to extract the k most important features from the images and then express each image as a linear combination of these features (we will use k=10). PCA will extract significant scene variations from the set of input images which maximize the covariance of the dataset. We will then look to use these coefficients as input to CCA. PCA will take as input a set of images I and will return three matrices $U \in \mathbf{R}^{m \times k}$, $S \in \mathbf{R}^{k \times k}$, and $V \in \mathbf{R}^{k \times n}$ where m is the length of a single image when expressed as a vector. U contains the k feature vectors, S is a diagonal matrix, and V contains the coefficients of each of the k feature vectors for each of the n images. We can thus create reconstructions of the images by multiplying U, S, and V back together.

MORE PCA MATH

The PCA coefficients for each image stored in V and our corresponding weather data $W \in \mathbf{R}^{y \times n}$ will be our input matrices for CCA. After running CCA, we will have projection matrices A and B. We can now use these to predict weather data from new images which were not included in the input for CCA. Given a new image i, we begin by obtaining the k PCA coefficients by projecting the image onto our existing basis vectors stored in U. We can now take those coefficients in a vector $\mathbf{v}$ and use them to predict the associated weather values $\mathbf{w}$ as follows:

$$\mathbf{w} = A\mathbf{v}B^{-1} \tag{2.1}$$

This is the key equation that is used to extract the inherent weather data from an image. We will now begin to apply these algorithms to actual data sets and present some results as well as additional information we can extract with regards to minimum size of the training set and the orientation of the camera.

Chapter 3

Results & Analysis

We consider two weather signals for our driving examples: wind velocity and vapor pressure. These two signals present unique challenges and opportunities. The effect of wind velocity is limited to locations in the scene that are affected by wind, such as flags and vegetation. On the other hand, vapor pressure may affect the scene in a more broad and subtle manner. Choosing two examples with such unique characteristics is a great way to test whether our algorithm is able to handle any variety of weather signals or if it can only handle certain types of measurements.

3.1 Wind Speed & Direction

Our first driving example of this method will be using wind velocity. Wind is a variable whose effects are only seen in certain local parts of the image; objects such s building and cars will be unaffected by changes in wind. In order to ensure that we could accurately predict the wind, we chose a camera which contained a flag (Figure 3.1). Our CCA projections are trained on 204 images collected between January 1 and February 11, 2009. In order to focus on variations in the scene due to weather, we only use images captured between 10 AM and 2 PM local time. By doing this we can successfully remove most of the variation caused by time of day and the resulting shadows. The wind data is made up of a wind speed and a direction in degrees, which we convert to north/south and east/west components, and was collected from the closest weather station to the camera.

Figure 3.1: Some sample images from camera #194 of the AMOS database located in Decatur, IN. The presence of a flag on top of the school building is key to our ability to predict wind speed and direction.

Based on this data, we would expect the two dimensions of the CCA projection matrix A to predict the north/south and east/west components of the wind speed.After running CCA, we can project matrix A onto our feature vectors U from the PCA analysis of the images to visualize the canonical features extracted by CCA. As we see in Figure 3.2(a), CCA clearly identifies the position of the flag as the crucial indicator of wind speed. Furthermore, we can also notice slight variations in the tree positions, which also are affected by wind speed. The projection of the second basis vector, which can be seen in Figure 3.2(b) is far less accurate and does not yield an accurate prediction of the other component of the wind speed. This indicates that we can only accurately predict wind speed along one of the two components. While this is not a favorable result, it is plausible and agrees with our assumptions; the flag captured in a 2D image can clearly only predict wind speed along one vector.

We can now use equation 2.1 to infer the magnitude of the wind velocity on 102 images collected between February 11 and March 17, 2009 which were not used in the training of the CCA. Figure 3.3 shows a plot of the ground truth values for wind speed as well as the predicted values using CCA. The associated images below the plot correspond to the filled markers and clearly indicate that our wind speed predictions not only agree with the ground truth values but also directly correlate with the direction of the flag. These results, along with the scatter plot in Figure 3.4

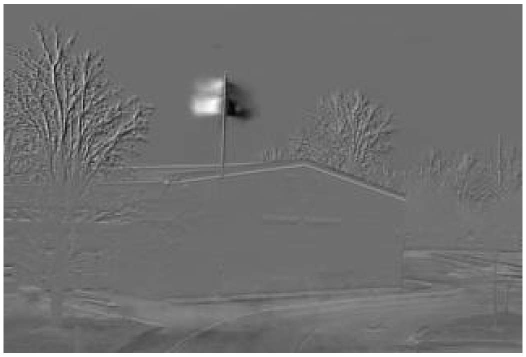

(a)

(b)

Figure 3.2: Figure 3.2(a) shows the projection of the first basis vector from CCA onto the original image space. It is clear to see that the position of the flag and the trees are the major variations. Figure 3.2(b) shows the projection of the second basis vector and is far less accurate than the first.

strongly supports our belief that wind speed along a given vector can be predicted based on the position of the flag ($r = 0.61759$).

Although we are unable to predict both components of the wind speed, there is still some more information we can extract from our results. Namely, we can use the known actual wind velocity vectors along with our predicted wind speed along some unknown vector to solve for the direction of that vector. We do this by solving a simple matrix equation of the form $Ax = b$ where $A \in \mathbf{R}^{n\times 2}$ are the known wind speeds in north/south and east/west components and $b \in \mathbf{R}^{n\times 1}$ are the predicted wind speeds along an unknown vector which will be perpendicular to x. Thus, solving for x will yield the vector perpendicular to the direction the flag blows in our camera. Figure 3.5 shows a scatter plot which visualizes the relationship between the actual and predicted wind speeds, along with the line solved for using the above equation. The same line is shown below overlaid onto an actual satellite image of the camera location.

3.2 Vapor Pressure

The second example will consider the weather signal of vapor pressure, which is the contribution of water vapor to the overall atmospheric pressure and is measured in

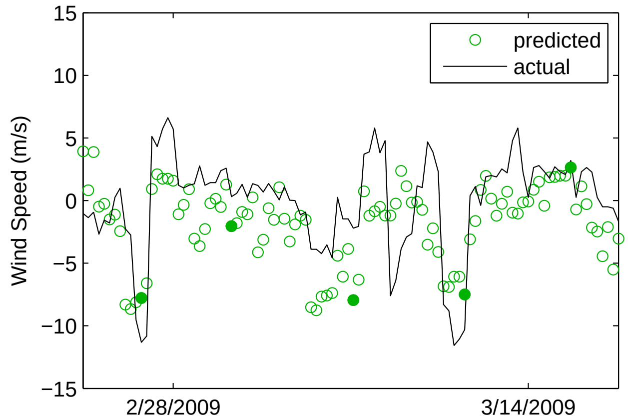

(a)

(b)

Figure 3.3: Predicted wind speed values and corresponding ground truth values in meters/seconds shown in Figure 3.3(a). Each image in Figure 3.3(b) is associated with one of the filled markers in the plot above.

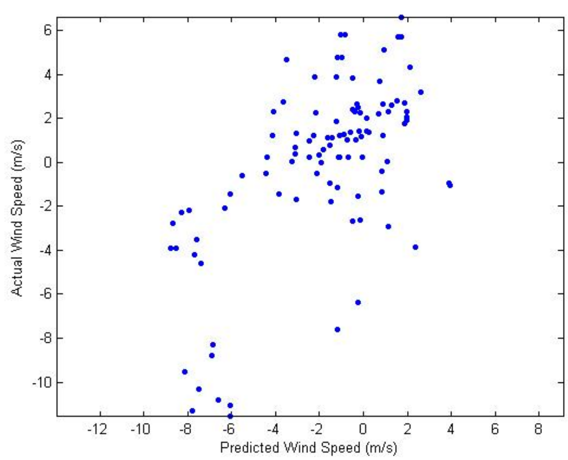

Figure 3.4: Scatter plot of predicted wind speed values vs. actual wind speed values. ($r = 0.61759$)

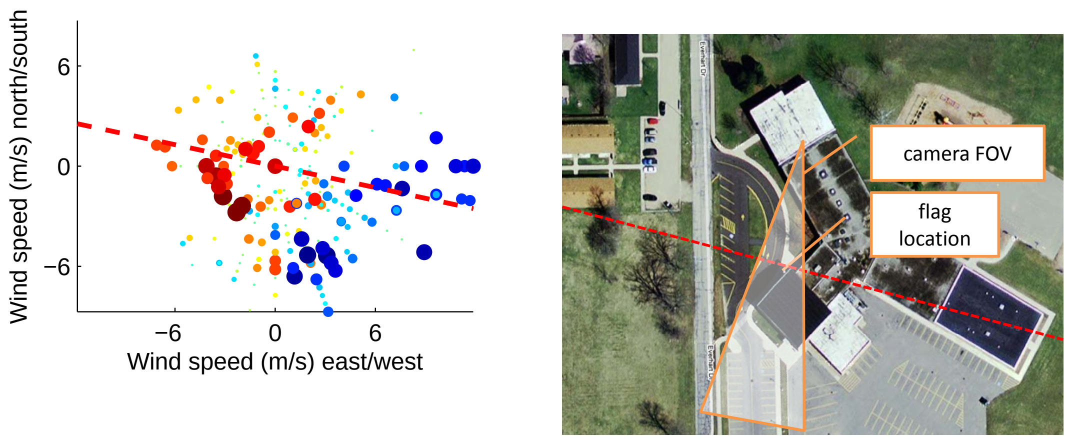

(a) (b)

Figure 3.5: Further analysis of the wind speed predictions provides a way for us to predict the axis along which the flag is blowing. In Figure 3.5(a) the size and color of each marker is determined by the predicted wind speed and the location of each marker is determined by the north/south and east/west components of the actual wind speed at the same time. The dashed red line is the normal to the projection axis determined by running linear regression between the predict and actual values. Figure 3.5(b) shows this axis overlaid on a Google Maps image with the field of view crudely estimated by hand.

Figure 3.6: Some sample images from camera #619 of the AMOS database located in Houston, TX. We focus on the visibility of the distant skyline of buildings as well as the presence of clouds to help us predict vapor pressure.

millibars. We note that since this is a 1-dimensional signal, unlike wind velocity, running CCA is essentially equivalent to linear regression. We chose a camera containing a distant skyline of buildings as well as a view of the sky and horizon (Figure 3.6). Our hypothesis is that as vapor pressure increases, the overall clarity of the distant skyline will decrease. The primary challenge with vapor pressure as opposed to wind speed is that it is a signal which effects the entire scene as opposed to a localized area, and is not quite as easy to comprehend visually.

The CCA projections for this example were trained on 198 images captured from January 1 to February 19, 2009. Once again, we only consider images between 10 AM and 2 PM as a way to ignore variations due to time of day.

Unfortunately, when we run the algorithm exactly as described above, we get poor results that do not correlate very strongly with what we expect to change with vapor pressure. As we see in Figure 3.7(a), the reprojection of the single dimension of CCA does not yield a very convincing image. It appears that the CCA projection has identified the position of the sun against the buildings as one of the important factors, which does not have anything to do with vapor pressure. Despite CCA identifying this seemingly unrelated signal, we get a decent correlation ($r = 0.59968$) between actual and predicted values, as seen in Figure 3.8(a). In order to improve our predictions

(a) (b)

Figure 3.7: The projections of the CCA basis vector computed with the regular and gradient images, respectively. Figure 3.7(a) does not identify a feature which actually correlates strongly with vapor pressure. However, when using the gradient image instead in Figure 3.7(b) we find that the CCA basis clearly identifies the visibility of the skyline as an indicator of vapor pressure, which agrees with our hypothesis.

and identify a relevant feature in the image, we replace the original images with their gradient magnitude images, which are computed as follows:

$$I_g = \sqrt{\frac{dI}{dx}^2 + \frac{dI}{dy}^2} \tag{3.1}$$

The gradient images will tend to focus on edges and other major changes in the images. The projection of the CCA basis we find when using these gradient images can be found in Figure 3.7(b) and, as we can see, clearly focuses on the visibility of the edges of the buildings, which is what we hypothesized would change with vapor pressure. Additionally, we get a stronger correlation between the actual and predicted values when using the gradient image ($r = 0.73684$).

Further analysis of our results indicate that we are correctly predicting vapor pressure and not some other signal which happens to correlate strongly with vapor pressure. Figure 3.9 shows the time series predicted vapor pressure data along with the ground truth values. We see that high vapor pressure measurements clearly indicate more cloudy days, which is exactly what we expect. This example also gives us a chance to identify one failure mode of our algorithm. On March 12, there was such a heavy fog that it obscured the entire scene, making it impossible to accurately predict

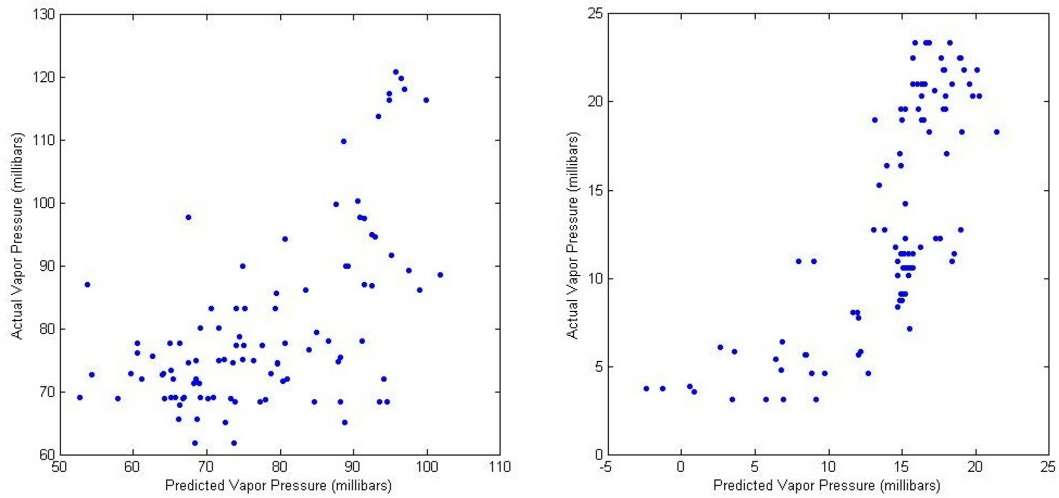

(a) (b)

Figure 3.8: Scatter plots of the predicted vs. actual vapor pressures (in millibars) computed with the regular and gradient images, respectively. While the correlation with the regular images (Figure 3.8(a), $r = 0.59968$) is not poor, there is a noticeable improvement when using the gradient images (Figure 3.8(b), $r = 0.73684$).

vapor pressure. This is an unavoidable failure mode as the algorithms depend on the appearance of the image and nothing else to predict the weather. Despite this failure mode, it is clear that our algorithm is able to successfully predict vapor pressure given a reasonable image of the scene.

3.3 Error Analysis

A standard question that must be asked of any machine learning algorithm is: how large of a training dataset is necessary to build an strong model? A strong model is on that can predict our given weather data both accurately *and* precisely. That is, our predictions from novel data have small error residuals and are not biased in one direction or the other. The combination of accuracy and precision is a strong argument that our model is truly predicting weather data and not some other signal from the image that is similar to the weather. The goal now is to find the minimum number of data samples which we need to build such a model.

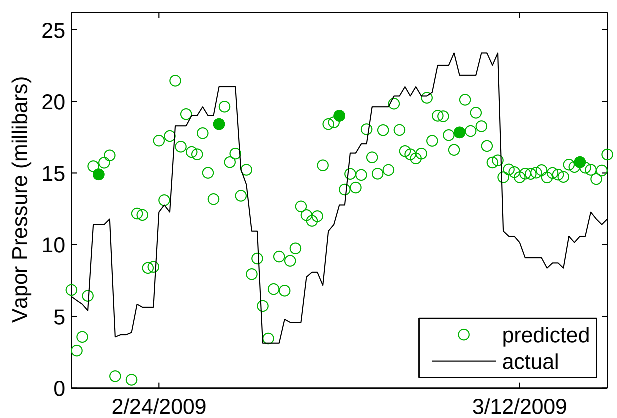

(a)

(b)

Figure 3.9: Predicted wind speed values and corresponding ground truth values in millibars shown in Figure 3.9(a). Each image in Figure 3.9(b) is associated with one of the filled markers in the plot above. The poor predictions on March 12 are due to heavy fog which obscured the entire scene and left water on the optics.

Prior work [1] using Monte Carlo simulations has suggested that CCA requires the size of the training dataset to be between 40 and 60 times the number of variables being used in correlation analysis. While this may be true for general cases, we will argue here that a far smaller amount is required if the samples sufficiently cover the distribution of possible values.

ADD CHARTS, SIZE ANALYSIS, ETC

Chapter 4

Conclusion

Chapter 5

Future Work

Appendix A

Camera Information

Appendix B

Weather Data

References

[1] Robert S. Barcikowski and James P. Stevens. A monte carlo study of the stability of canonical correlations, canonical weights and canonical variate-variable correlations. In *Multivariate Behavioral Research*, volume 10:3, pages 353–364, 1975.

[2] M. Borga, H. Knutsson, and T. Landelius. Learning canonical correlations. In *SCIA10*, Lappeenranta, Finland, June 1997. SCIA.

[3] H. Hotelling. Relations between two sets of variates. In *Biometrika*, volume 28, pages 321–377, 1936.

[4] Nathan Jacobs, Walker Burgin, Richard Speyer, David Ross, and Robert Pless. Adventures in archiving and using three years of webcam images. In *IEEE Workshop on Internet Vision (CVPR 2009)*, Miami, FL, June 2009. (to appear).

[5] Nathan Jacobs, Nathaniel Roman, and Robert Pless. Consistent temporal variations in many outdoor scenes. In *IEEE Computer Society Conference on Computer Vision and Pattern Recognition (CVPR 2007)*, Minneapolis, MN, June 2007.

[6] Nathan Jacobs, Nathaniel Roman, and Robert Pless. Toward fully automatic geo-location and geo-orientation of static outdoor cameras. In *IEEE Workshop on Applications of Computer Vision (WACV 2008)*, Copper Mountain, CO, January 2008.

[7] Nathan Jacobs, Scott Satkin, Nathaniel Roman, Richard Speyer, and Robert Pless. Geolocating static cameras. In *Proc. IEEE International Conference on Computer Vision (ICCV)*, Rio De Janiero, Brazil, October 2007.

[8] Dongge Li, Nevenka Dimitrova, Mingkun Li, and Ishwar K. Sethi. Multimedia content processing through cross-modal association. In *MULTIMEDIA '03: Proceedings of the eleventh ACM international conference on Multimedia*, pages 604–611, New York, NY, USA, 2003. ACM.

[9] S.G. Narasimhan, C. Wang, and S.K. Nayar. All the Images of an Outdoor Scene. In *Europian Conference on Computer Vision (ECCV)*, volume III, pages 148–162, May 2002.

[10] National Oceanic and Atmospheric Administration. Historical weather data archives, April 2009. http://data.nssl.noaa.gov/.

Vita

Richard Speyer

Date of Birth	October 11, 1986
Place of Birth	Johannesburg, South Africa
Degrees	B.S. Computer Science, May 2009 M.S. Computer Science, May 2009
Professional Societies	Association for Computing Machinery
Publications	N. Jacobs, S. Satkin, N. Roman, R. Speyer, and R. Pless. Geolocating static cameras. In *Proc. IEEE International Conference on Computer Vision*, Oct. 2007. N. Jacobs, W. Burgin, R. Speyer, D. Ross, and R. Pless. Adventures in Archiving and Using Three Years of Webcam Images. In *IEEE Workshop on Internet Vision (CVPR 2009)*, Jun. 2009. (to appear)

May 2009

Predicting Weather from Image Sequences, Speyer, M.S. 2009